

Production of negative hydrogen ions using a low-pressure reflex discharge source

Emil I. Toader

Abstract In this paper we analyze the possibility to use the reflex discharge plasma as a volume source of negative hydrogen ions. The basic internal parameters like the temperature T_e and the density n_e of the electrons, the density n_+ of the positive hydrogen ions, the density n_- of the negative hydrogen ions, and the negative ion fraction n_-/n_e are measured and discussed. The operating conditions are optimized within the pressure range 0.1–10 Pa, the discharge power 20–140 watt, and the magnetic field 0–150 gauss. The experiment shows that the enhanced magnetic ionization is the most effective within the pressure range from 0.7 to 4.0 Pa. When $p \approx 1$ Pa the cold electron temperature T_e is 0.77 eV, the cold electron density n_e is $4.2 \times 10^{18} \text{ m}^{-3}$ and the negative ion density n_- is as high as $0.8 \times 10^{17} \text{ m}^{-3}$. The negative ion fraction n_-/n_e increases from 1.4% for $p = 0.1$ Pa to almost 2.2% within the pressure range 1–4 Pa. The positive ion density scales with the power, while the negative ion density and the negative ion fraction seems to saturate at higher power levels.

Key words magnetized plasma • negative ions • plasma sources

Introduction

The future success of neutral beam heating for the next generation of fusion machines depends on the development of negative hydrogen/deuterium ion beams of high intensity. Unlike the positive hydrogen ions, negative hydrogen ions have the advantage that only a single species H^-/D^- exists, so all the particles in the neutralized beam will have the same energy. If a plasma neutralizer is used for H^- neutralization, efficiencies of over 80% can be achieved. When a photodetachment neutralizer is used, the efficiency may increase to almost 100%, since the photon energy can be selected to detach the weakly bound outer electron of the H^- ion, but not to ionize the resulting hydrogen atom. A number of other applications like particle acceleration and solid state technology require high brightness negative ion sources. Almost all accelerators use partially ionized plasmas as devices for transporting charged beams. At present, the negative hydrogen production techniques are based mainly on the volume production technique [1–14] and surface conversion technique [18]. In the “volume” source, the negative ions are formed by dissociative attachment between vibrationally excited gas molecules and very cold electrons ($T_e \leq 1$ eV) within the plasma volume. The “surface” source forms negative ions by double electron capture or by sputtering when an H^+ ion strikes a negatively biased surface coated with a cesium or barium film. Roughly, a fraction of 0.1 or less of the incoming positive flux is reemitted as negative ions but the transverse velocity of these ions is large.

E. I. Toader
Faculty of Physics,
University of Bucharest,
Box MG-11, 077125 Bucharest-Magurele, Romania,
Tel.: +40 21 4574636 ext. 134, Fax: +40 21 4574521,
E-mail: milan_toader@yahoo.co.uk

Received: 25 August 2005
Accepted: 21 November 2005

Recently, we reported on a new type of plasma source [15–17]. Its design, construction and analysis were prompted by the necessity to obtain high density plasmas using low dissipated power. The source is obtained as a hybrid between a Penning discharge and a hollow cathode discharge. The main advantage of this cold-cathode, direct current driven negative ion source over the filament discharge ones is the absence of short life components, e.g., the filaments themselves.

The magnetic field enhanced hollow cathode effect leads to plasmas with: (a) high density; (b) high uniformity; (c) three groups of electrons; and (d) no electric field. These characteristics, coupled with those of an efficient negative ion source, that is, the existence of one group of high energy electrons for generating the plasma and the ro-vibrationally excited molecules, and another group of cold electrons for producing H^- ions by dissociative electron attachment, have stimulated our interest in the analysis of this reflex discharge plasma as a potential source of negative ions. To our knowledge, this is the first time when the reflex discharge plasma is analyzed as a possible source of negative ions. Particularly, we are interested here in the internal parameters in the case of the hydrogen reflex discharge plasma.

The electron energy distribution function EEDF, the electron temperature T_e , the electron density n_e , and the positive ion density n_i are measured using the Langmuir probe method and the Druyvesteyn procedure, coupled with a suitable software [5, 12]. The diagnostic method based on laser beam photodetachment of negative ions and detection of detached electrons by an electrostatic probe [1] is used to measure the density n_- of the hydrogen negative ions. The operating conditions are optimized for n_e , T_e , n_i , n_- and n_-/n_e within the pressure range 0.1–10 Pa, the discharge power 20–140 W, and the magnetic field 0–150 G.

Experimental set-up and reflex discharge mechanism

The non-magnetic stainless steel discharge chamber is of cylindrical form, 300 mm long and 200 mm inside diameter. It is enclosed at each end by detachable, non-magnetic stainless steel flanges (Fig. 1). One port has a quartz window with a diameter of 80 mm for visual observation of the discharge. The other port is used for placing a Langmuir probe within discharge space and moving it to different positions. The two 100 mm diameter, plane-parallel, stainless steel cathodes are on extensions which penetrate but are insulated from the end flanges, via O-ring gaskets. This allows the inter-cathode gap to be varied from 10 to 100 mm, and the cathodes to be powered and water-cooled. The non-magnetic stainless steel cathodes can be covered by aluminum or by copper discs, as experimental conditions required. The grounded, non-magnetic stainless steel anode, in the form of a ring with 102 mm inside diameter, 10 mm width and 2.0 mm thickness, is placed symmetrically with respect to the two plane-parallel flanges. This system allows the gap between each cathode and the anode to be varied independently. The power was provided by a 1800 V and 0.4 A direct current

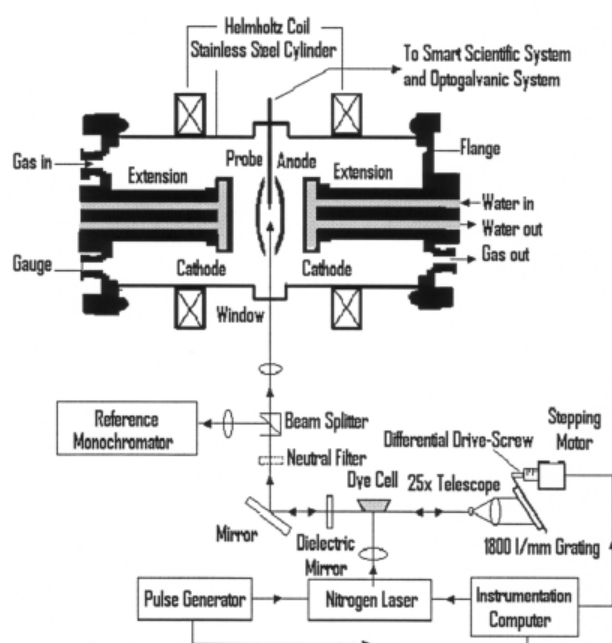


Fig. 1. Schematic representation of the experiment with the reflex plasma source and auxiliary equipment used for plasma diagnostic.

power supply, which can work either in constant current mode and constant voltage mode. The discharge current and voltage were read in the usual way using digital meters.

The magnetic field is created by means of two Helmholtz coils placed symmetrically relative to the middle of the discharge vessel. The average distance between the two coils is 15 cm, equal to the average radius of the coils. The current through the Helmholtz coils is electronically stabilized, and is insensitive to the change of the coil resistance due to the heat of the coils. The uniformity of the magnetic field was checked with a Hall probe and was found to have an uniformity better than one percent over the whole discharge region, in agreement to the theoretic data used to design the Helmholtz coil. The electron gyration radius is smaller than the diameter of the discharge cylindrical vessel. Consequently, the residence time and path length of electrons in the plasma is increased, and so is the probability of them causing ionizing collisions.

An oil sealed mechanical pump backing a turbomolecular pump evacuates the discharge chamber to an ultimate vacuum less than or equal to 10^{-7} Pa. The reflex discharge is run within the pressure range 0.1–10 Pa, buffering the pump and flowing hydrogen at a flow rate of 2 to 40 sccm. The gas pressure is measured using a Pirani gauge and a Penning gauge. The discharge is run in all cases for an inter-cathode distance of 40 mm, a magnetic field within the range 0–150 G, and the anode placed symmetrically in respect to the two plane cathodes. The anode is grounded to the discharge chamber and the two cathodes are connected to the direct-current power supply at the same potential.

When considering the mechanism of the reflex discharge, one must keep in mind the geometry of the device where the two plane-parallel cathodes act like

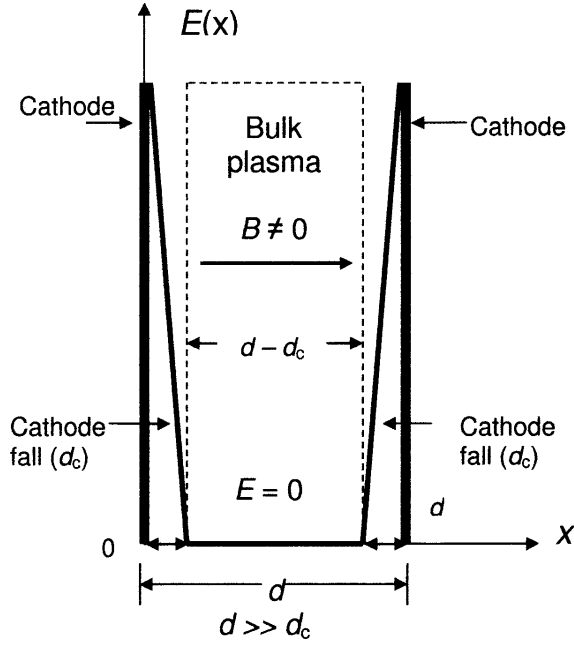


Fig. 2. Schematic representation of the reflex discharge cavity, with the axial electric field within the bulk plasma and cathode fall regions.

a cavity for the electrons (Fig. 2). The primary electrons are emitted from either one of the two symmetric plane-parallel cathodes due to secondary electron emission process. They are accelerated in the corresponding thin cathode dark space, which is less than one millimeter thick up to the energies corresponding to the cathode fall potential U_c , which is almost equal to the discharge voltage of a few hundred volts. These primary electrons with energies of a few hundred electronvolt penetrate the two joined negative glows that form the bulk plasma region, losing part of their energy by excitation and ionization. The bulk plasma region occupies almost the whole space between the two opposing plane cathodes. The ionization process produces cold electrons. The secondary electrons are those primary electrons that have lost energy in numerous collisions with neutrals and ions.

The primaries are emitted perpendicularly to the cathode surface. They move parallel to the magnetic field towards the opposite cathode fall region, penetrate to a depth which depends on the energy they lost within the bulk plasma, and are reflected back toward the first cathode fall region. This is the so-called pendulum effect (pendulum electrons), responsible for the hollow cathode effect (HCE). Due to the pendulum effect there is an enhancement of the ionization rate, and the fraction of the plasma ions incident on each cathode surface is increased, and more primary electrons are released due to the ion bombardment. Unlike the ordinary hollow cathode discharge, in this reflex discharge there is an axial magnetic field with a double role. First, the residence time of the electrons within the bulk plasma region is increased, by increasing the number of reflections of a primary electron between the two plane-parallel cathodes, and this causes a further enhancement of the ionization rate. Second, the radial loss of ions to the chamber wall is decreased

and so more ions from the bulk plasma hit the cathodes releasing more primaries. The consequence is a higher plasma density and an increased discharge current at relatively low discharge voltages.

Diagnostic technique

The movable cylindrical Langmuir probe is inserted into the plasma region from a lateral port of the stainless steel processing chamber. It is positioned perpendicularly to the magnetic field, and can be moved in the radial direction. The thin wire probe tip is made of tungsten and is 6 mm long and 125 μm in diameter. The probe circuit included a grounded anode as a reference electrode. The probe is connected to a Scientific System probe control unit, and a software similar to that, described elsewhere [5, 12, 15–17], is used for data acquisition. The collisionless conditions for using a cylindrical Langmuir probe in magnetized plasma is described as a function of four parameters, i.e., the electron free mean path λ_e , the probe radius r_p , the plasma Debye length λ_D , and the Larmor radius r_L , that is

$$(1) \quad \lambda_e \gg r_p \gg \lambda_D$$

and

$$(2) \quad r_L \gg r_p$$

The plasma Debye length is given by the formula

$$(3) \quad \lambda_D = (\epsilon_0 k_B T_e / e^2 n)^{1/2}$$

and the mean Larmor radius for electrons having a Maxwellian energy distribution is

$$(4) \quad r_L = (\pi m_e k_B T_e / 2)^{1/2} / eB$$

where: ϵ_0 is the permittivity of vacuum; k_B is the Boltzmann constant; m_e is the electron mass; e is the electron charge; T_e is the electron temperature; n is the plasma density, and B is the strength of the magnetic field. At the typical operating pressures of our experiments, corresponding to the low-pressure case, the mean free paths is longer than 10 mm, the Debye length is $\approx 10 \mu\text{m}$ and the Larmor radius is $\approx 1.0 \text{ mm}$ for electrons, so the conditions (1) and (2) are satisfied. With a good approximation, we can neglect the influence of the magnetic field on the probe voltage-current characteristics $I(V)$, where I is the probe current, $V = V_p - V_s$, V_p is the probe potential, and V_s is the plasma potential at the position of the probe.

The electron temperature T_e is obtained using the formula

$$(5) \quad T_e = \frac{2}{3} \langle \epsilon \rangle = \frac{2}{3n_e} \int_0^\infty \epsilon f(\epsilon) d\epsilon$$

The electron density n_e is obtained by integrating the electron energy distribution function $f(\epsilon)$

$$(6) \quad n_e = \int_0^{\infty} f(\varepsilon) d\varepsilon$$

where, according to the Druyvesteyn procedure

$$(7) \quad f(\varepsilon) = 2(2m_e)^{1/2}(eA)^{-1}e^{1/2}d^2I_p/dV^2$$

and where A is the probe surface area and e is the electron energy. The EEDF, $f(\varepsilon)$, is obtained from the probe voltage-current characteristics using the Druyvesteyn procedure, and the second derivative is computed from probe current measurements using an energy resolution of 0.2 eV.

The ion density n_i is obtained from the ion saturation current branch of the probe characteristics, using the computer controlled Langmuir probe system. The expression of the ion current to the probe $I(V)$, defined as a function of the probe voltage V , is

$$(8) \quad I_i(V) = en_i r_p (2\pi k_B T_e / m_i)^{1/2} f(r_p / \lambda_D, eV / k_B T_e)$$

where: m_i is the mass of the positive ion; $f(r_p / \lambda_D, eV / k_B T_e)$ is the ion current expansion factor computed in the zero-ion temperature limit [12].

To measure the density n_- of the hydrogen negative ions in the plasma volume we use the method developed by Bacal [1]. The electron affinity for hydrogen is 0.745 eV, hence for photodetachment of H^- ions to occur, photons with energy greater than 0.745 eV are required. The principle of this method is to destroy all the negative ions in the plasma region illuminated by a laser beam of appropriate energy by pumping the electron from the ground state into the continuum, that is $H^- + h\nu \rightarrow H + e^-$. Photodetachment produces an increase in the electron density without an immediate increase of the positive ion density. Thus, by simply collecting these extra electrons with a positively biased Langmuir probe, the fraction of negative ions which are destroyed during the laser pulse, $\Delta n_- / n_-$, is

$$(9) \quad \frac{\Delta n_-}{n_-} = 1 - \exp\left[-\frac{E}{A_L} \cdot \frac{\sigma}{h\nu}\right]$$

where: E is the laser pulse energy; A_L is the laser beam area; σ is the cross section for photodetachment of H^- ions; $h\nu$ is the laser photon energy. At high pulse energy the photodetachment fraction $\Delta n_- / n_-$ is essentially 100% and the relative H^- ion density n_- / n_e can be determined from the change in the probe electron current

$$(10) \quad \frac{n_-}{n_e} = \frac{\Delta n_e}{n_e} = \frac{\Delta i^-}{i_{dc}^-}$$

where: Δi^- is the amplitude of the photodetachment pulse current; i_{dc}^- is the dc probe current; n_e is the electron density measured separately using the computerized Langmuir probe technique described above; Δn_e is the increase in the electron density directly after the laser pulse, this is equivalent to the negative ion density.

To check the accuracy of the photodetachment optical galvanic measurements as a function of the laser energy and wavelength we use a tunable dye-laser within the wavelength range 450–500 nm (Fig. 1). The cross section for the photodetachment of the electrons from H^- is almost half of its maximum of 4×10^{-17} cm². A pulsed nitrogen laser (a wavelength of 337.1 nm and a pulse width of 6 ns), delivering about 200 kW peak power, can pump coumarin 1 in a dye-laser cavity, at a maximum repetition rate of 2 kHz internally and externally pulsed. An 1800-lines/mm diffraction grating, used with a 25× beam-expanding telescope in the optical cavity, gives a linewidth of almost 0.019 nm within the wavelength range 430–520 nm. The wavelength drive consists of a differential screw which rotates the grating. A stepping motor interfaced with a computer served to advance the wavelength in 0.003 nm. The dye-laser beam with a diameter of ≈ 2.5 mm, repetition rate of 10 Hz, and a maximum output energy per unit area of ≈ 0.20 J/cm², is aligned coaxially with the cylindrical probe which is biased at an appropriate positive potential (electron saturation branch of the V - I probe characteristics) to collect the electrons liberated by photodetachment of the negative ions. A suitable electronic arrangement allows the detection of only the liberated electrons and not the continuous current to the probe from the free electrons in the plasma. Neutral filters are used to check that the experiment is run in the conditions where the photodetachment fraction is independent of the dye laser pulse energy.

There are different statistical errors associated with the measured plasma parameters. These have been estimated by comparing measurements made at different times under the same conditions (pressure, gas flow rate and total input power). The relative standard uncertainty is less than 10% for electron temperature, 6% for plasma potential and floating potential, and 15% for electron density and ion density. Taking into account the uncertainty of the probe surface area of ca. 5%, the total relative standard uncertainty for electron density and ion density is estimated to be 20%.

Results. Discussion

The geometric parameters were varied to obtain a bulk plasma volume as big as possible. Consequently, the experiment was run up to the maximum inter-cathode distance $d = 100$ mm. The experiment shows that for $d > 60$ mm the two negative glow regions do not overlap, and the HC effect disappears. To obtain optimum discharge conditions, the experiment must be run at an inter-cathode distance of the resonance cavity of 40 mm, at a gas flow rate of 20 sccm. Since the inter-cathode distance d is much bigger than the cathode fall distance d_c , we may consider that the whole volume of the bulk plasma appears as a cage for the electrons. All the discharge voltage-current characteristics show that the enhanced magnetic ionization is more effective at higher discharge currents, and higher magnetic fields.

The experimental electron energy distribution functions show invariable two electron temperatures, i.e., one temperature corresponding to the cold group

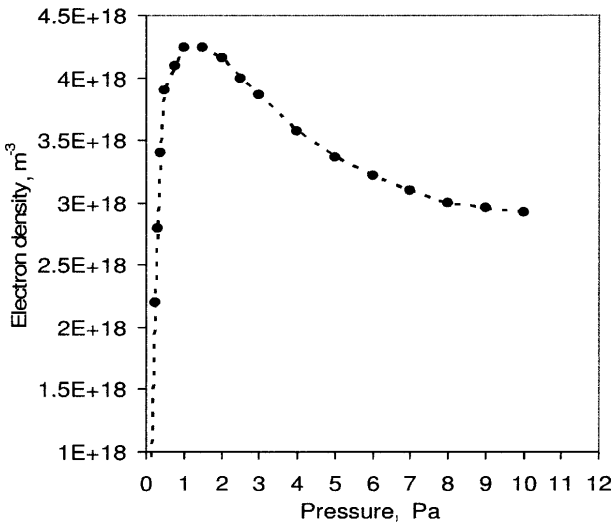


Fig. 3. Dependence of electron temperature measured at the centre of the discharge chamber for $P = 100$ W, $B = 100$ G and $\Phi = 20$ sccm, and $d = 40$ mm on pressure.

of electrons (bulk electrons) and the other temperature corresponding to hot group of electrons. Here, we are interested in the temperature of the bulk electrons responsible for the dissociative attachment that leads to the appearance of negative ions. The data obtained for T_e are presented in Fig. 3 as a function of the gas pressure p for the dissipated power $P = UI = 100$ W. Here, U is the discharge voltage and I is the discharge current. In the same experimental conditions, we measured also the dependence of the electron density n_e on the gas pressure p . The results obtained are presented in Fig. 4. We observe a very quick increase of the electron density within the pressure range from 0.1 Pa to 0.8 Pa, and a smooth decrease within the pressure range from 4 Pa to 10 Pa. The electron density n_e peaks for $p \approx 1.0$ Pa. These data show that the enhanced magnetic ionization is the most effective

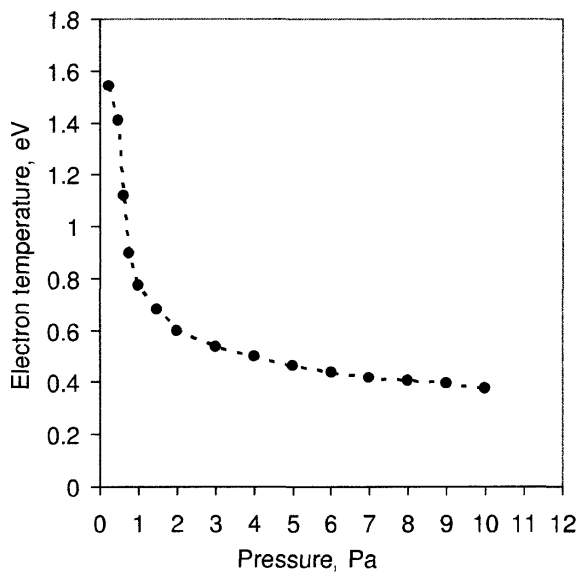


Fig. 4. Dependence of electron density measured at the centre of the discharge chamber for $P = 100$ W, $B = 100$ G and $\Phi = 20$ sccm, and $d = 40$ mm on pressure.

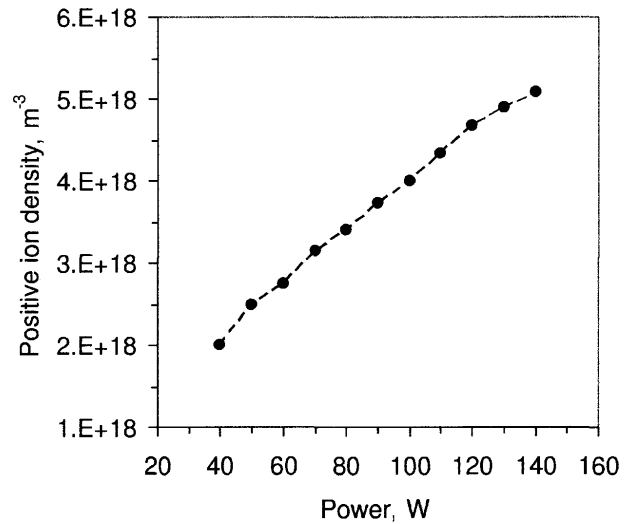


Fig. 5. Dependence of ion density measured at the centre of the discharge chamber for $p = 1.0$ Pa, $B = 100$ G and $\Phi = 20$ sccm, and $d = 40$ mm on power.

within the pressure range from 0.7 to 4.0 Pa. Dependence on power of the ion density measured at the centre of the discharge chamber for $p = 1.0$ Pa, $B = 100$ G is presented in Fig. 5. Based on the results reported by Bacal *et al.* [2], we considered that H_3^+ is the dominant ion species in these plasmas. Indeed, the production of H_2^+ and H^+ ions is due to ionization from collisions of primary electrons (fast electrons, e_{fast}) with hydrogen molecules and hydrogen atoms, respectively. The reactions involved are: $e_{\text{fast}} + H_2(v=0) \rightarrow H_2^+(v) + 2e$; $H_2^+(v) + H_2(v=0) \rightarrow H_3^+(v') + H$, and $e_{\text{fast}} + H \rightarrow H^+ + 2e$. The interaction cross section that leads to the appearance of H_3^+ can be as high as 10^{-14} cm² [6]. Mullan and Graham [13] reported values of the positive ion fraction as high as 97% for H_3^+ .

Figure 6 shows the measurement of the negative ion density n_- (right side), and the negative ion fraction n_-/n_e (left side) as a function of source pressure for

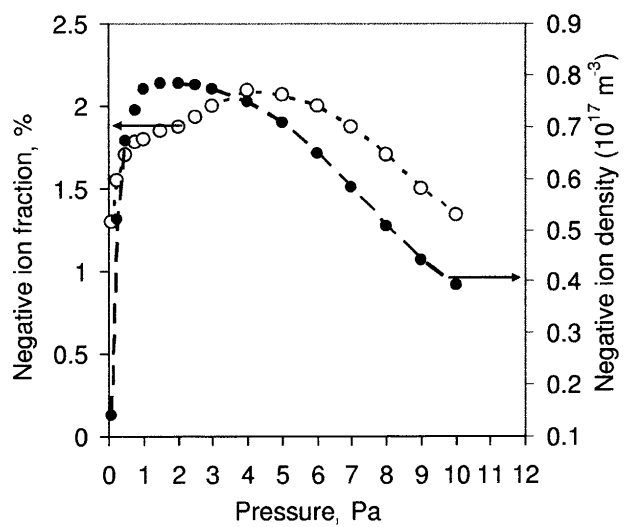


Fig. 6. Dependence of negative ion fraction (left) and negative ion density (right) measured at the centre of the discharge chamber for $P = 100$ W, $B = 100$ G, and $\Phi = 20$ sccm, and $d = 40$ mm on pressure.

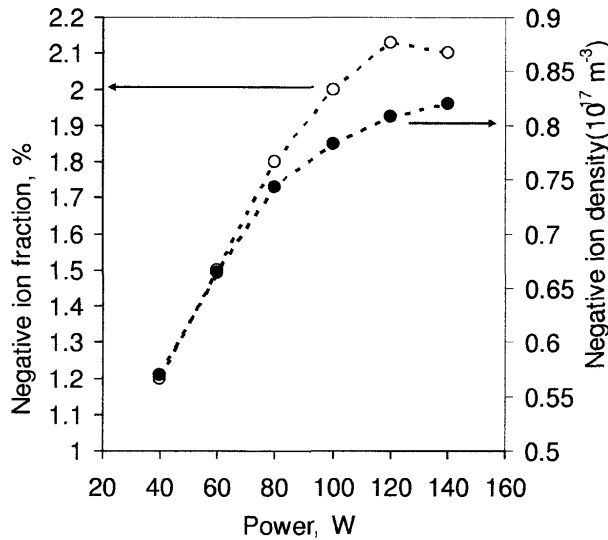
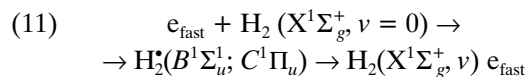


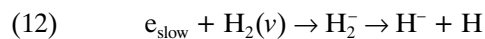
Fig. 7. Dependence of negative ion fraction (left) and negative ion density (right) measured at the centre of the discharge chamber for $p = 1.0$ Pa, $B = 100$ G, and $\Phi = 20$ scm, and $d = 40$ mm on power.

$P = 100$ W and $B = 100$ G. At low pressure, we see a sharp increase of n_- up to $0.8 \times 10^{17} \text{ m}^{-3}$ when $p \approx 1$ Pa. A further increase of the pressure p up to 10 Pa leads to a decrease of the negative ion density. On the other hand, the negative ion fraction increases from 1.4% for $p = 0.1$ Pa to almost 2.2% within the pressure range 1–4 Pa, and then decreases to 1.34% for $p = 10$ Pa. In Fig. 7, are presented the values obtained for the negative ion density and negative ion fraction as a function of power. If the positive ion density scales with the power P (see Fig. 5), the negative ion density and the negative ion fraction seems to saturate at higher power levels.

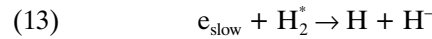
The reason for an optimum pressure of around 1.0 Pa in the reflex discharge negative ion source can be explained considering the mechanisms of producing negative hydrogen ions. Dissociative attachment from vibrationally excited H_2 molecules in their ground electronic state is the main accepted mechanism for H^- negative-ion production in volume plasmas [11]. The first step is the formation of vibrationally excited molecules $\text{H}_2(v)$ via the radiative decay of the B and C excited molecule state



The electron energy threshold for this process is around 13 eV and the cross section is maximal at about 25 eV. Once the vibrational molecular state is formed, it is long lived unless a second fast electron collision occurs leading usually to dissociation or if it collides with the wall and jumps to a lower vibrational quantum level. If a slow electron collides with this vibrational molecule, dissociative attachment occurs forming an H^- ion via the short-lived H_2^- state



The cross section for this process increases from about 10^{-22} cm^2 to 10^{-16} cm^2 as v changes from 0 to 6. It then saturates at $4 \times 10^{-16} \text{ cm}^2$ for H_2 up to the highest vibrational level. The electron energy for a maximum rate coefficient is 0.6–0.8 eV for all vibrational levels. Detailed analyses of the volume sources show that up to 85% of the H^- production from processes (11) and (12) is obtained via $\text{H}_2(X^1\Sigma_g^+, v > 5)$ states [4]. Another channel of enhancing the concentration of negative ions H^- relies on dissociative attachment from Rydberg states [7, 8, 14]. This process can be described as



where: H_2^* represents a hydrogen molecule in a high-lying excited Rydberg state.

The dependence of the internal plasma parameters on gas pressure (Figs. 3, 4, and 6) evidences three pressure ranges, e.g., $p < 1.0$ Pa, $1.0 \text{ Pa} < p < 4.0$ Pa, and $p > 4.0$ Pa. The dependence of the positive ion density (Fig. 5), and negative ion density (Fig. 7) on power P is quite different at the highest power levels. Consequently, the experimental results in Figs. 3–7 must be discussed and analyzed considering both the reflex discharge mechanism and the mechanisms of producing negative hydrogen ions. As discussed in paragraph 2, when a voltage is applied between the two cathodes and anode, a reflex discharge develops and cathode fall regions form over the cathode surfaces. The reflex discharge consists of two distinct regions, that is, the bulk plasma region, which is essentially electric field free, and the cathode fall region, where all the applied voltage is concentrated (Fig. 2). There is only the primary group of electrons within the cathode fall regions, while in the bulk plasma region there are three groups of electrons, e.g., primary electron group, secondary electron group, and thermalized (bulk/cold) electron group. Almost all electrons are in the energy range $0 \leq w \leq E^*$ (elastic energy range, E^* is the threshold of inelastic processes, and w the electron kinetic energy). They are generated during ionization of the gas particles, have a Maxwell energy distribution, ensure quasi-neutrality of the plasma and carry no current. These electrons lose their energy essentially through electron-electron and electron-atom/molecule elastic collisions, stepwise excitation and ionization, and are responsible for the dissociative attachment process that leads to the H^- production (processes (12) and (13)). On contrary, the primary electrons (or fast electrons) have energies higher than one hundred of electronvolt, carry almost all the discharge current, and are responsible for the production of excited molecules (process (11)). Secondary electrons have the average energy 4 to 6 times higher than the average energy of the cold electrons. We distinguish between the cold/thermalized electron group and the secondary electron group since within the energy range 0 to 15 eV the electron energy distribution function is bi-Maxwellian, clearly evidencing the two groups of electrons [15–17].

The experiment shows that for $p < 1.0$ Pa the discharge voltage is higher than that corresponding to the gas pressure around 1.0 Pa. To maintain the dissipated power P constant, the discharge current must

be lowered. But at lower current levels the hollow cathode effect and the magnetic enhancement ionization are less effective. Since in the reflex discharge plasma the discharge current is due to the fast electrons (primary electrons), lower discharge current levels means also lower values for the fast electron density, and consequently lower values for the cold electron density (see Fig. 3), and higher values for the cold electron temperature (see Fig. 4). According to the reaction (10), fewer fast electrons within the plasma region means less vibrationally excited molecules, and lower values for the negative ion density, as showed in Fig. 6. Since the hollow cathode effect and the magnetic enhancement ionization are less effective, the cold electron density decreases and the cold electron temperature increases. According to reactions (12) and (13), the H^- production decreases. On the other hand, for $p > 4.0$ Pa the increase of the discharge voltage is small, so the variation of the discharge current is smooth and this fact is evidenced by the smooth variation of the electron density in Fig. 4. Since $T_e < 0.6$ eV (Fig. 3), the attachment process is less favorable, so the negative ion density decreases.

The fact that the positive ion density scales with the power P when $p = 1.0$ Pa, is a consequence of the reflex discharge mechanism. The quasi-neutrality condition implies $n_+ = n_e + n_- \approx n_e$. The experiment proves that the optimum discharge conditions are obtained for pressure values around 1.0 Pa. Within the power range $50 < P < 150$ W any power increase is due mainly to the increase of the discharge current (hollow cathode effect), so $n_+ \propto I$. When $I \rightarrow 0.4$ A the electron temperature decreases and has values lower than 0.6 eV. The H^- production process is less favorable, and the negative ion density and the negative ion fraction decrease as showed in Fig. 7.

Conclusion

The experiment shows that the reflex plasma discharge can be considered as a potential source of negative hydrogen ions. The main advantage of this cold-cathode, direct current driven negative ion source over the filament discharge ones is the absence of short-life components, e.g., the filaments themselves. The electron energy distribution functions measured within the energy range from 0 to 15 eV show invariable two electron temperatures, corresponding to the cold group of electrons and the hot group of electrons, respectively. The optimum discharge conditions are obtained for pressure values around 1.0 Pa, in agreement with the acceptable upper limits of almost 0.7 Pa reported for hydrogen tandem ion sources [10]. When $p \approx 1$ Pa the negative ion density n_- is as high as $0.8 \times 10^{17} \text{ m}^{-3}$, the cold electron density n_e is $4.24 \times 10^{18} \text{ m}^{-3}$ and the cold electron temperature T_e is 0.77 eV. The negative ion fraction n_-/n_e increases from 1.4% for $p = 0.1$ Pa to almost 2.2% within the pressure range 1–4 Pa. The positive ion density scales with the power, while the negative ion density and the negative ion fraction seems to saturate at higher power levels.

Acknowledgment This work was supported by the International Atomic Energy Agency – Grant No. 12411/RO, and the CNCSIS, Romania Grant No. 33379/04.

References

1. Bacal M (2000) Photodetachment diagnostic techniques for measuring negative ion densities and temperatures in plasmas. *Rev Sci Instrum* 71:3981–4006
2. Bacal M, Bruneteau AM, Graham WG, Hamilton GW, Nachman M (1981) Pressure and electron temperature dependence of H^- density in a hydrogen plasma. *J Appl Phys* 52:1247–1254
3. Bacal M, Hamilton GW (1979) H^- and D^- production in plasmas. *Phys Rev Lett* 42:1538–1540
4. Berlemont P, Skinner DA, Bacal M (1993) Negative ion volume production model: State of the experimental confirmation. *Rev Sci Instrum* 64:2721–2728
5. Bretagne J, Graham WG, Hopkins MB (1991) A comparison of experimental and theoretical electron energy functions in a multicusp ion source. *J Phys D Appl Phys* 24:668–671
6. Bruneteau AM, Bacal M (1985) Effect of positive and negative ion energies on H^- destruction by mutual neutralization in low-pressure plasmas. *J Appl Phys* 57:4342–4348
7. Celiberto R, Laricchiuta A, Lamanna UT, Janev RK, Capitelli M (1999) Electron-impact excitation cross sections of vibrationally excited $X^1\Sigma^+_g H_2$ and D_2 molecules to Rydberg states. *Phys Rev A* 60:2091–2103
8. Hassouni K, Gicquel A, Capitelli M (1998) The role of dissociative attachment from Rydberg states in enhancing H^- concentration in moderate and low-pressure H_2 plasma sources. *Chem Phys Lett* 290:502–508
9. Hershcovitch AI, Johnson BM, Kovarik VJ *et al.* (1984) Neutralization of multi-MeV light negative ions by plasma neutralizers. *Rev Sci Instrum* 55:1744–1747
10. Hiskes JR (1994) Optimum extracted H^- and D^- current densities from gas-pressure-limited high-power hydrogen/deuterium tandem ion sources. *Rev Sci Instrum* 65:1219–1221
11. Holmes AJT (1992) Negative hydrogen ion beams. *Plasma Phys Controlled Fusion* 34:653–676
12. Hopkins MB, Graham WG (1986) Langmuir probe technique for plasma parameter measurement in a medium density discharge. *Rev Sci Instrum* 57:2210–2217
13. Mullan AA, Graham WG (1991) Study of the discharge of a multicusp ion source operating with H_2 and D_2 . *J Phys D Appl Phys* 24:1533–1540
14. Pinnaduwa LA, Christophorou LG (1993) H^- formation in laser-excited molecular hydrogen. *Phys Rev Lett* 70:754–757
15. Toader EI (2004) Experimental electron energy distribution functions in argon, nitrogen and oxygen high-density and low-pressure reflex and microwave plasma sources. *Plasma Sources Sci Technol* 13:646–653
16. Toader EI, Covlea V (2005) Enhanced magnetic ionization in hydrogen reflex discharge plasma source. *Rev Sci Instrum* 76:033502
17. Toader EI, Covlea V, Graham WG, Steen PG (2004) High density and low temperature direct current reflex plasma source. *Rev Sci Instrum* 75:382–386
18. Wimmer E, Freeman AJ, Weinert M *et al.* (1982) Cesium of W(001): Work function lowering by multiple dipole formation. *Phys Rev Lett* 48:1128–1131